

Exotic Acoustic-Edge and Thermal Scaling in Disordered Hyperuniform Networks

Yang Jiao^{1,2}

¹*Materials Science and Engineering, Arizona State University, Tempe, AZ 85287*

²*Department of Physics, Arizona State University, Tempe, AZ 85287*

(Dated: October 30, 2025)

We develop a first-principles theory for the vibrational density of states (VDOS) and thermal properties of network materials built on stationary correlated disordered point configurations. For scalar (mass–spring) models whose dynamical matrix is a distance-weighted graph Laplacian, we prove that the limiting spectral measure is the pushforward of Lebesgue measure by a Fourier symbol that depends only on the edge kernel f and the two-point statistics g_2 (equivalently the structure factor S). For hyperuniform systems with small- k scaling $S(k) \sim k^\alpha$ and compensated kernels, the VDOS exhibits an algebraic *pseudogap* at low frequency, $g(\omega) \sim \omega^{2d/\beta-1}$ with $\beta = \min\{4, \alpha + 2\}$, which implies a low-temperature specific heat $C(T) \sim T^{2d/\beta}$ and a heat-kernel decay $Z(t) \sim t^{-d/\beta}$, defining a spectral dimension $d_s = 2d/\beta$. This hyperuniformity-induced algebraic edge depletion could enable novel wave manipulation and low-temperature applications. Generalization to vector mechanical models and implications on material design are also discussed.

Disorder hyperuniform (DHU) many-body systems lack conventional long-range order as in an amorphous material, yet they possess a “hidden order” manifested as complete suppression of normalized infinite-wavelength density fluctuations like crystals [1, 2]. Recently, a wide spectrum of equilibrium [3, 4] and non-equilibrium [5–7] many-body systems, in both classical [8–13] and quantum mechanical [14–21] varieties, have been identified to possess the property of disordered hyperuniformity. Other examples include certain biological systems [22–24], driven non-equilibrium systems [25–31], active-particle fluids [32–36], and dynamic random organizing systems [37–40]. Novel DHU materials have been engineered that can possess superior properties compared to their crystalline counterpart, such as high-degree of isotropy and robustness against defects [41–48].

Hyperuniformity is characterized by a local number variance $\sigma_N^2(R)$ associated with a spherical window of radius R in \mathbb{R}^d that grows more slowly than the window volume in the large- R limit [1, 2], i.e., $\lim_{r \rightarrow \infty} \sigma_N^2(R)/R^d = 0$. Equivalently, the static structure factor vanishes in the infinite-wavelength (or zero-wavenumber) limit, i.e., $\lim_{|\mathbf{k}| \rightarrow 0} S(\mathbf{k}) = 0$, where \mathbf{k} is the wavenumber and $S(\mathbf{k})$ is related to the pair-correlation function $g_2(\mathbf{r})$ via $S(\mathbf{k}) = 1 + \rho \int e^{-i\mathbf{k} \cdot \mathbf{r}} [g_2(\mathbf{r}) - 1] d\mathbf{r}$ and $\rho = N/V$ is the number density of the system. For statistically isotropic systems, the structure factor only depends on the wavenumber $k = |\mathbf{k}|$. The small- k scaling behavior of $S(k)$, i.e., $S(k) \sim k^\alpha$ determines the large- R asymptotic behavior of $\sigma_N^2(R)$, based on which all DHU systems can be categorized into three classes: $\sigma_N^2(R) \sim R^{d-1}$ for $\alpha > 1$ (class I); $\sigma_N^2(R) \sim R^{d-1} \ln(R)$ for $\alpha = 1$ (class II); and $\sigma_N^2(R) \sim R^{d-\alpha}$ for $0 < \alpha < 1$ (class III), where α is the hyperuniformity exponent [2].

Recent numerical studies on hyperuniform glasses and designed disordered materials [49–52] report depleted low-frequency modes, modified heat capacities, and in some models apparent low-frequency gaps [53]. In con-

trast to ordered network systems [54, 55], what has been missing for disordered systems is a compact analytic relation that predicts the low-frequency vibrational density of states (VDOS) and associated thermal exponents directly from the structural statistics of the disordered underlying point configuration (e.g., distribution of the particle centers).

Here we provide such a relation for scalar mass–spring networks by developing a first-principles theory. Specifically, the VDOS is a pushforward of Lebesgue measure by a symbol $\Lambda_L(k)$ of the scalar dynamical Laplacian L , determined only by the edge kernel f and pair statistics g_2 (or equivalently structure factor S). For compensated kernels (see definition below), hyperuniformity yields a universal algebraic *pseudogap* at the acoustic edge with exponent fixed by the small- k scaling of $S(k)$. Our framework bridges random geometric graph theory and the statistical mechanics of hyperuniform point processes, and offers parameter-free predictions testable against numerical results and inspires novel material design.

Scalar dynamical matrix as a distance-weighted Laplacian. Let $\mathbf{x}_1, \dots, \mathbf{x}_N \in \Omega \subset \mathbb{R}^d$ be points from a stationary, isotropic process of number density $\rho = N/\text{Vol}(\Omega)$ and pair correlation function $\rho^{(2)}(\mathbf{x}, \mathbf{y}) = \rho^2 g_2(|\mathbf{x} - \mathbf{y}|) = \rho^2 g_2(r)$, where $r = |\mathbf{x} - \mathbf{y}|$ is the Euclidean distance between point \mathbf{x} and \mathbf{y} . Consider a nonnegative, rapidly decaying radial kernel $f(r)$ defining weighted edges between sites, which also defines a graph based on the point configuration. Examples of $f(r)$ include inverse power functions, Gaussian, or exponential kernels. The connectivity/adjacency matrix A has entries

$$A_{ij} = \begin{cases} f(|\mathbf{x}_i - \mathbf{x}_j|), & i \neq j, \\ 0, & i = j. \end{cases} \quad (1)$$

In this work, we focus on the “scalar elasticity” problem based on the graph (i.e., a network of scalar “springs”),

i.e.,

$$Lu_n = \lambda u_n \quad (2)$$

where L is the (mass-normalized) scalar dynamical matrix and $\lambda_n = \omega_n^2$ is the eigen value of the matrix, with ω_n being the vibration frequencies. We note in this setting, L is also the graph Laplacian, i.e., $L = D - A$, with $D = \text{Diag}(d_1, \dots, d_n)$ and $d_i = \sum_j f(|\mathbf{x}_i - \mathbf{x}_j|)$ [56, 57]. Thus the entries of the Laplacian is given by

$$L_{ij} = \begin{cases} -f(|\mathbf{x}_i - \mathbf{x}_j|), & i \neq j, \\ \sum_{m \neq i} f(|\mathbf{x}_i - \mathbf{x}_m|), & i = j. \end{cases} \quad (3)$$

L is symmetric, positive semidefinite and its eigenvalues $\lambda_n \geq 0$ are related to mode frequencies by $\omega_n^2 = \lambda_n$. Denote by $\varphi_L(\lambda)$ the limiting eigenvalue density (per site in the infinite N limit) of L , the vibrational density of states (VDOS) is given by [58, 59]

$$g(\omega) = 2\omega \varphi_L(\lambda) \Big|_{\lambda=\omega^2}. \quad (4)$$

DOS from two-point statistics. Consider the static structure factor of the point configuration $S(k) = 1 + \rho \hat{h}(k)$ where $\hat{h}(k)$ is the Fourier transform of the total correlation function $h(r) = g_2(r) - 1$, the operator L converges (in the thermodynamic limit, in the sense of empirical spectral measures) to a translation-invariant convolution operator with symbol (i.e., the Fourier transform of the operator) [60–62]

$$\Lambda_L(k) = \bar{d} - \Lambda_A(k) \quad (5)$$

where

$$\bar{d} = \Lambda_A(0) = \rho \int f(r) g_2(r) d^d r \quad (6)$$

and

$$\Lambda_A(k) = \rho \widehat{f g_2}(k) = \rho \hat{f}(k) + \frac{1}{(2\pi)^d} (\hat{f} * (S - 1))(k), \quad (7)$$

and $\Lambda_A(k)$ is the symbol of the adjacency matrix operator. For any bounded continuous test function ϕ , the convergence of the empirical spectral measures is stated as [63, 64]:

$$\lim_{N \rightarrow \infty} \frac{1}{N} \mathbb{E}[\text{Tr } \phi(L)] = \frac{1}{(2\pi)^d} \int \phi(\Lambda_L(k)) d^d k, \quad (8)$$

and the limiting density of eigenvalues is

$$\varphi_L(\lambda) = \frac{1}{(2\pi)^d} \int \delta(\lambda - \Lambda_L(k)) d^d k. \quad (9)$$

where $\delta(\cdot)$ is the Dirac delta function. Equations (4)–(9) connects vibrational spectra prediction to two-point information.

Hyperuniform acoustic-edge scaling. We now consider a power-law small- k scaling of the structure factor, i.e., $S(k) \sim A_H |k|^\alpha$ as $k \rightarrow 0$ with $\alpha > 0$, and assume that \hat{f} is analytic near $k = 0$. Then the non-analytic contribution from $S - 1$ affect the symbol near the acoustic edge as follows (see SI for details):

$$\Lambda_L(k) = C_2 |k|^2 + C_{2+\alpha} |k|^{2+\alpha} + C_4 |k|^4 + o(|k|^4), \quad (10)$$

where $C_2 = \frac{\rho}{2d} M_2$ and $C_4 = \frac{\rho}{8d(d+2)} M_4$ and $M_n = \int_{\mathbb{R}^d} r^n f(r) d^d r$; $C_{2+\alpha}$ is the coefficient associated with the $S(k)$ contribution, which is given in SI.

It can be seen from Eq.(10) that for typical kernels (Gaussian, exponential, inverse power-law), the k^2 term is dominating. Keeping only the leading term $\Lambda_L(k) \approx \frac{\rho M_2}{2d} k^2$ near the edge, Eq. (9) for small λ yields

$$\varphi_L^D(\lambda) \approx \frac{S_{d-1}}{2(2\pi)^d} \left(\frac{\rho}{2d} M_2 \right)^{-d/2} \lambda^{d/2-1} \quad (11)$$

where $S_{d-1} = 2\pi^{d/2}/\Gamma(d/2)$ is the d -dimensional solid angle. For VDOS, this yield

$$g^D(\omega) = 2\omega \varphi_L(\omega^2) \sim \omega^{d-1} \quad (12)$$

which is the universal Debye exponent for the low-frequency state [58, 65]. In this case, the effect of hyperuniformity ($\alpha > 0$) is masked by the analyticity of the kernel function.

Here we consider the so-called *compensated kernels*, i.e., one that satisfies

$$M_2 = \int_{\mathbb{R}^d} r^2 f(r) d^d r = 0 \quad (13)$$

and $M_4 > 0$, which contributes to the Laplacian symbol with k^4 term. Examples of such systems include bending-dominated elastic medium, i.e. the discrete analog of the Kirchhoff–Love plate or Euler–Bernoulli beam [66] and 2D materials [67]. An example of such compensated kernel is

$$f_c(r) = e^{-(r/a)^2} - \eta e^{-(r/b)^2}, \quad (14)$$

where $\eta = \left(\frac{a}{b}\right)^{d+2}$ and $0 < a < b$ are length scale parameters.

For a Poisson distribution of points, $S(k) = 1$ and the spectra symbol of the adjacency and Laplacian operators reduce to $\Lambda_A(k) = \rho \hat{f}(k)$ and $\Lambda_L(k) = \bar{d} - \Lambda_A(k) = \rho [\hat{f}(0) - \hat{f}(k)]$, respectively. With the compensated kernel Eq.(14), the leading term is $\Lambda_L(k) \approx C_4 k^4$, which yields

$$\varphi_L^P(\lambda) \sim \frac{S_{d-1}}{4(2\pi)^d} C_4^{-\frac{d}{4}} \lambda^{\frac{d}{4}-1} \quad (15)$$

and

$$g^P(\omega) \sim \frac{S_{d-1}}{2(2\pi)^d} C_4^{-d/4} \omega^{\frac{d}{2}-1} \sim \omega^{\frac{d}{2}-1} \quad (16)$$

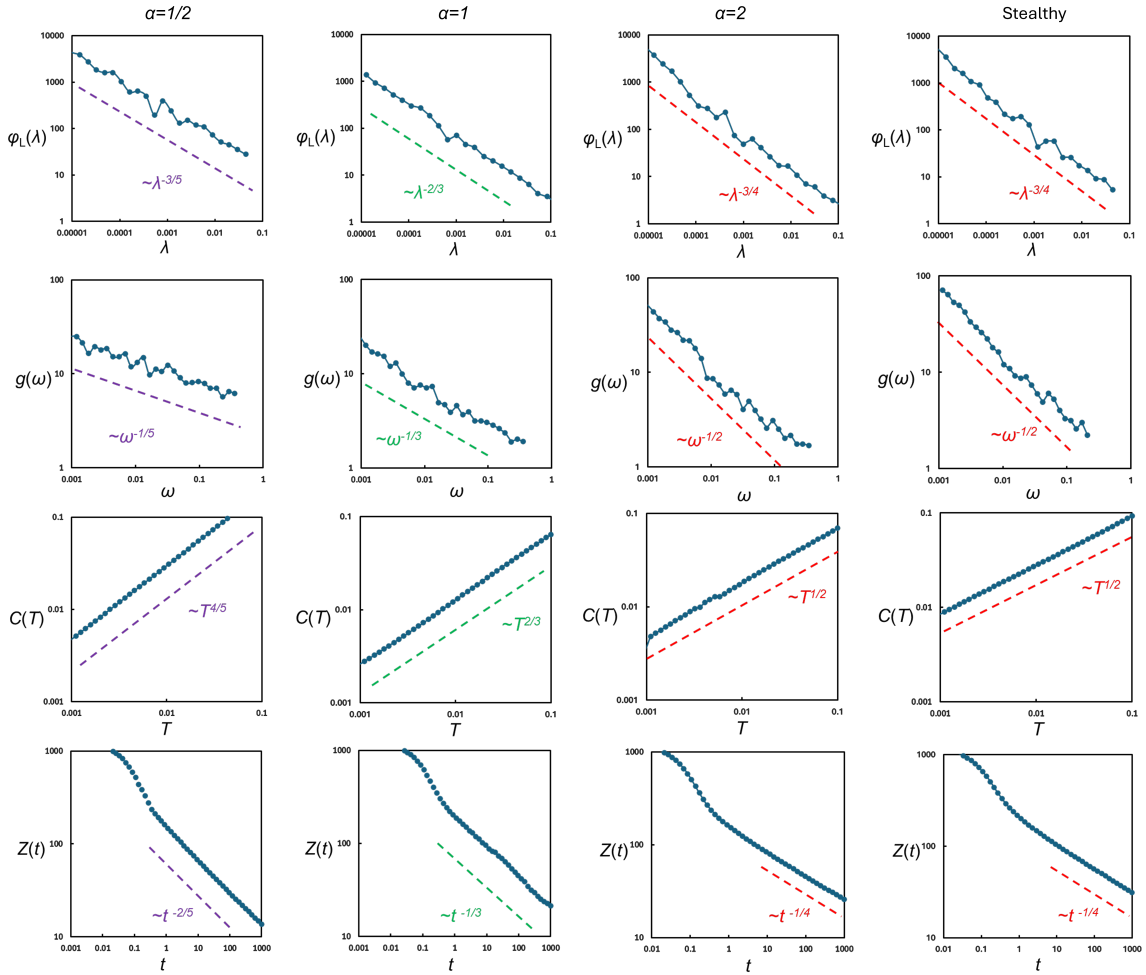


FIG. 1: Comparisons of theoretical predictions for eigen value distribution $\varphi_L(\lambda) \sim \lambda^{d/\beta-1}$, VDOS $g(\omega) \sim \omega^{2d/\beta-1}$, heat capacity $C(T) \sim T^{2d/\beta}$ (per node, with unit k_B) and heat kernel $Z(t) \sim t^{-d/\beta}$ with numerical results of a variety of hyperuniform systems with $\alpha = 1/2, 1, 2$ and stealthy systems in 1D with $N = 10,000$ points in a unitary periodic box and the compensated kernel (14) with $a = 0.002$ and $b = 0.004$. The scaling behaviors of the reported quantities are not sensitive to choice of a and b values. The results are obtained by averaging over 10 independent realizations for each case.

For hyperuniform systems ($0 < \alpha < 2$) with compensated kernels, the leading order term is $\Lambda_L(k) \approx C_{2+\alpha} k^{2+\alpha} + o(k^4)$. Plugging this into Eq. (9) yields the following scaling of the edge states:

$$\varphi_L^H(\lambda) \sim \frac{S_{d-1}}{(2\pi)^d} \frac{1}{\beta} C_\beta^{-d/\beta} \lambda^{\frac{d}{\beta}-1} \quad (17)$$

and, via (4), the VDOS near the edge is given by

$$g^H(\omega) \sim \frac{S_{d-1}}{(2\pi)^d} \frac{2}{\beta} C_\beta^{-d/\beta} \omega^{\frac{2d}{\beta}-1} \sim \omega^{\frac{2d}{\beta}-1} \quad (18)$$

where $\beta = \min\{4, 2 + \alpha\}$.

Eq. (18) indicates that, for a hyperuniform system in ($d \geq 2$) with hyperuniformity exponent $0 < \alpha < 2$, the spectrum touches zero, yet the density of states near

the edge vanishes algebraically with a stronger power law than the Poisson and general Debye systems. For $d = 1$, a stronger depletion at the edge is also manifested, e.g., as the slower diverging the zero- k states. Because $\Lambda_L(k)$ is a continuous scalar function on a connected Brillouin zone, the spectrum of L is the essential range of Λ_L , i.e., a *single connected band* touching 0 at $k = 0$. Thus the scalar model produces an *algebraic pseudogap* (depletion) at the edge, not a true forbidden interval.

We numerically test our theoretical predictions using one-dimensional point configurations, including Poisson (see Supporting Information) and several classes of disordered hyperuniform (DHU) systems with exponents $\alpha = 1/2, 1, 2$, as well as stealthy patterns, each containing $N = 10,000$ points. For every case, ensemble averages

are obtained over 10 independent realizations. The DHU configurations are generated via the collective coordinate method [68]. Figures 1 top two rows respectively compare the theoretical predictions with numerical results for the edge behavior of $\varphi_L(\lambda)$ and $g(\omega)$, showing excellent agreement across all systems.

We note that the stronger power-law depletion of low-frequency modes in hyperuniform networks effectively trims the soft tail of the spectrum, which can significantly impact the elastic moduli, wave responses and vibrational noise floors. For elastic moduli, non-affine correction terms scale like $\int g(\omega)\Gamma(\omega)/\omega^2 d\omega$; thus, depletion of low- ω modes lowers these corrections, pushing moduli closer to their affine (stiffer) values and reducing sample-to-sample variability. For wave response, the scarcity of ultra-soft modes, together with suppressed long-wavelength density fluctuations, reduces large-scale scattering/attenuation in the acoustic range. Moreover, quantities weighted by $1/\omega^2$ (e.g. thermal displacement noise) decrease as the low- ω DOS is thinned, enabling lower noise and potentially higher precision engineering.

Hyperuniform thermal exponents. Consider the internal energy of harmonic oscillators, i.e.,

$$U(T) = \int_0^\infty \hbar\omega \frac{1}{e^{\hbar\omega/k_B T} - 1} g(\omega) d\omega \sim A_\beta \int_0^\infty \hbar\omega \frac{\omega^p}{e^{\hbar\omega/k_B T} - 1} d\omega \quad (19)$$

where $p = \frac{2d}{\beta} - 1$. Simplifying Eq. (19) yields the low- T scaling (see SI for details):

$$U(T) \sim T^{2d/\beta+1}. \quad (20)$$

The heat capacity $C(T)$ is then obtained by differentiating the internal energy, i.e.,

$$C(T) = \frac{dU}{dT} \sim T^{2d/\beta}, \quad \beta = \min\{4, 2 + \alpha\} \quad (21)$$

For Poisson systems, we have $\beta = 4$, which leads to the low- T scaling of heat capacity $C^P(T) \sim T^{d/2}$. Hyperuniform systems with $0 < \alpha < 2$ have $\beta = 2 + \alpha < 4$, giving

$$C^H(T) \sim T^{2d/(2+\alpha)}, \quad (22)$$

with a *higher* power than $T^{d/2}$ and therefore a much stronger low- T suppression. In $d = 3$, e.g. $\alpha = 1$ (jammed particle packings [6]) yields $C^H(T) \sim T^2$ (vs. $T^{3/2}$ in Poisson systems), implying orders-of-magnitude reduction at millikelvin–kelvin scales. Therefore, such hyperuniform materials can enable fast thermal response (for fast thermometry and pulsed operation), thermal management by design (e.g., engineering $S(k)$ to target specific $C(T)$ curves for cryogenic subsystems), and enhance sensitivity and bandwidth at low T calorimetry and bolometry. Figure 1 third row compares the theoretical predictions with numerical results for the low- T

scaling of the heat capability $C(T)$ and excellent agreement across all systems is observed.

Finally, we note that the Laplacian L also governs the diffusion/heat transport on network, i.e.,

$$d\mathbf{T}(t)/dt = -L\mathbf{T}(t) \quad \mathbf{T}(t) = e^{-Lt}\mathbf{T}(0) \quad (23)$$

Thus, the same spectra used for vibrations also controls relaxation on networks. We consider the heat trace

$$Z(t) = \text{Tr } e^{-tL}, \quad (24)$$

which governs the relaxation in the system. For large t , the heat trace possesses the following form

$$Z(t) = \int_0^\infty e^{-t\lambda} \varphi_L(\lambda) d\lambda \quad (25)$$

which is dominated by small λ . Plugging in Eq. (17)

$$Z(t) \sim \frac{S_{d-1}}{(2\pi)^d} \frac{1}{\beta} C_\beta^{-d/\beta} \int_0^\infty e^{-t\lambda} \lambda^{\frac{d}{\beta}-1} d\lambda = \frac{S_{d-1}}{(2\pi)^d} \frac{1}{\beta} C_\beta^{-d/\beta} \Gamma\left(\frac{d}{\beta}\right) t^{-d/\beta}. \quad (26)$$

which indicates the large- t scaling $Z(t) \sim ct^{-d/\beta}$, defining a spectral dimension $d_s = 2d/\beta$. Figure 1 fourth row shows the comparison of our theory to numerical data, which again shows excellent agreement.

For hyperuniform systems with $0 < \alpha < 2$, $\beta = 2 + \alpha < 4$, $Z^H(t) \sim t^{-d/(2+\alpha)}$ decays faster than the Poisson systems with $Z^P(t) \sim ct^{-d/4}$, implying quicker equilibration, shorter mixing times, and less thermal memory. This result is consistent with a recent study on the diffusion spreadability, characterizing transport in two-phase media, which indicates hyperuniform systems can achieve exponentially fast homogenization [45].

Discussion. For *Stealthy hyperuniform* (SHU) system possessing $S(k) = 0$ for $|k| < K$ (effectively $\alpha \rightarrow \infty$), the non-analytic contribution from $S - 1$ is absent and the analytic kernel term controls the edge. Hence $\beta = 4$ for compensated kernels, $g(\omega) \propto \omega^{d/2-1}$ with $C(T) \propto T^{d/2}$.

For *antihyperuniform* (AHU) point sets with $S(k) \sim k^\alpha$ and $-d < \alpha < 0$, the correlation cusp dominates the analytic k^2 term [c.f. Eq.(10)] and renormalizes the small- k symbol to a *fractional order* $\Lambda_L(k) \sim k^\gamma$ with $\gamma = 2 + \alpha \in (0, 2)$, even for generic short-range kernels (no compensation needed). By phase-space counting this yields non-Debye edge exponents: $\varphi(\lambda) \sim \lambda^{d/\gamma-1}$, $g(\omega) \sim \omega^{2d/\gamma-1}$, $C(T) \sim T^{2d/\gamma}$, and $Z(t) \sim t^{-d/\gamma}$. Because $\gamma < 2$, AHU media exhibit a *stronger depletion* of acoustic-edge states than Debye, which is an apparently counter-intuitive result that follows from the more non-linear $k \mapsto \omega$ mapping of a softer (fractional) operator, not from increased “order.”

Recent numerical studies on hyperuniform glasses and designed disordered materials [49–52] report suppressed low-frequency VDOS, modified transport, and in some

over-jammed regimes gap-like windows. Our theory explains the *phonon-like* (acoustic) part via the two-point structure alone: (i) the depletion exponent at the acoustic edge is fixed by the small- k law of $S(k)$ through (18); (ii) the corresponding thermal exponents $C(T) \sim T^{2d/\beta}$ and $Z(t) \sim t^{-d/\beta}$ follow immediately; (iii) a true low-frequency gap requires a matrix-valued dynamical matrix (vector modes, resonant elements, or multi-sublattice structure), consistent with models where constraints or multi-component architectures are essential. Features attributed to “non-phononic” excitations (e.g., ω^4 modes in generic glasses) likely reflect disorder beyond two-point statistics, while our results isolate the universal, two-point-controlled contribution in hyperuniform networks.

Conclusions and outlook. Equations (8)–(18) provide a compact, predictive link from the *two-point* structural statistics of a disordered hyperuniform medium to its *vibrational spectrum* and *thermal* exponents. The theory requires only f and $S(k)$, readily accessible from scattering or simulations, and yields parameter-free predictions for universal exponents. We showed that disordered hyperuniform systems with $0 < \alpha < 2$ possess stronger depletion for deeper vibrational and thermal suppression. By prescribing the small- k form of the structure factor $S(k)$ (and a local coupling f), one can set the acoustic-edge law and thus the low-frequency vibrational spectrum and the low-temperature specific heat. This enables structure-factor engineering of materials: quieter phononic components and precision supports with fewer soft modes, and cryogenic/low-noise devices with reduced $C(T)$. Extending the pushforward framework to vector dynamical matrices is a natural next step; we expect the small- k non-analyticity of $S(k)$ to continue to control the acoustic-branch exponents, while additional branches and non-phononic modes provide model-specific corrections. Our results place recent numerical observations on a theoretical footing, delineating the universal role of hyperuniform two-point statistics and clarifying when genuine gaps require structure beyond a scalar distance-Laplacian.

Acknowledgments. This work was supported by the Army Research Office under Cooperative Agreement Number W911NF-22-2-0103.

[1] S. Torquato and F. H. Stillinger, Phys. Rev. E **68**, 041113 (2003).

[2] S. Torquato, Phys. Rep. **745**, 1 (2018).

[3] S. Torquato, G. Zhang, and F. H. Stillinger, Phys. Rev. X **5**, 021020 (2015).

[4] R. D. Batten, F. H. Stillinger, and S. Torquato, Phys. Rev. Lett. **103**, 050602 (2009).

[5] A. Gabrielli, M. Joyce, and F. S. Labini, Phys. Rev. D **65**, 083523 (2002).

[6] A. Donev, F. H. Stillinger, and S. Torquato, Phys. Rev. Lett. **95**, 090604 (2005).

[7] C. E. Zachary, Y. Jiao, and S. Torquato, Phys. Rev. Lett. **106**, 178001 (2011).

[8] R. Kurita and E. R. Weeks, Phys. Rev. E **84**, 030401 (2011).

[9] G. L. Hunter and E. R. Weeks, Rep. Prog. Phys. **75**, 066501 (2012).

[10] R. Dreyfus, Y. Xu, T. Still, L. A. Hough, A. G. Yodh, and S. Torquato, Phys. Rev. E **91**, 012302 (2015).

[11] D. Chen, X. Jiang, D. Wang, H. Zhuang, and Y. Jiao, Acta Materialia **246**, 118678 (2023).

[12] H. Zhang, X. Wang, J. Zhang, H.-B. Yu, and J. F. Douglas, arXiv preprint arXiv:2302.01429 (2023).

[13] A. Chremos and J. F. Douglas, Phys. Rev. Lett. **121**, 258002 (2018).

[14] R. P. Feynman and M. Cohen, Phys. Rev. **102**, 1189 (1956).

[15] Y. A. Gerasimenko, I. Vaskivskyi, M. Litskevich, J. Ravnik, J. Vodeb, M. Diego, V. Kabanov, and D. Mihailovic, Nat. Mater. **18**, 1078 (2019).

[16] S. Sakai, R. Arita, and T. Ohtsuki, arXiv preprint arXiv:2207.09698 (2022).

[17] G. Rumi, J. A. Sánchez, F. Elías, R. C. Maldonado, J. Puig, N. R. C. Bolecek, G. Nieva, M. Konczykowski, Y. Fasano, and A. B. Kolton, Phys. Rev. Res. **1**, 033057 (2019).

[18] J. A. Sánchez, R. C. Maldonado, N. R. C. Bolecek, G. Rumi, P. Pedrazzini, M. I. Dolz, G. Nieva, C. J. van der Beek, M. Konczykowski, C. D. Dewhurst, et al., Commun. Phys. **2**, 1 (2019).

[19] Y. Zheng, L. Liu, H. Nan, Z.-X. Shen, G. Zhang, D. Chen, L. He, W. Xu, M. Chen, Y. Jiao, et al., Sci. Adv. **6**, eaba0826 (2020).

[20] D. Chen, Y. Zheng, L. Liu, G. Zhang, M. Chen, Y. Jiao, and H. Zhuang, Proc. Natl. Acad. Sci. U.S.A. **118**, e2016862118 (2021).

[21] D. Chen, R. Samajdar, Y. Jiao, and S. Torquato, Proceedings of the National Academy of Sciences **122**, e2416111122 (2025).

[22] Y. Jiao, T. Lau, H. Hatzikirou, M. Meyer-Hermann, J. C. Corbo, and S. Torquato, Phys. Rev. E **89**, 022721 (2014).

[23] Z. Ge, Proc. Natl. Acad. Sci. USA **120**, e2306514120 (2023).

[24] Y. Liu, D. Chen, J. Tian, W. Xu, and Y. Jiao, Physical Review Letters **133**, 028401 (2024).

[25] D. Hexner and D. Levine, Phys. Rev. Lett. **114**, 110602 (2015).

[26] R. L. Jack, I. R. Thompson, and P. Sollich, Phys. Rev. Lett. **114**, 060601 (2015).

[27] J. H. Weijns, R. Jeanneret, R. Dreyfus, and D. Bartolo, Phys. Rev. Lett. **115**, 108301 (2015).

[28] M. Salvalaglio, M. Bouabdellaoui, M. Bollani, A. Benali, L. Favre, J.-B. Claude, J. Wenger, P. de Anna, F. Intonti, A. Voigt, et al., Physical Review Letters **125**, 126101 (2020).

[29] Ü. S. Nizam, G. Makey, M. Barbier, S. S. Kahraman, E. Demir, E. E. Shafiq, S. Galioglu, D. Vahabli, S. Hüsnügil, M. H. Güneş, et al., Journal of Physics: Condensed Matter **33**, 304002 (2021).

[30] Y. Zheng, M. A. Klatt, and H. Löwen, arXiv preprint arXiv:2310.03107 (2023).

[31] J. Wang, Z. Sun, H. Chen, G. Wang, D. Chen, G. Chen, J. Shuai, M. Yang, Y. Jiao, and L. Liu, Physical Review

Letters **134**, 248301 (2025).

[32] Q.-L. Lei, M. P. Ciamarra, and R. Ni, *Sci. Adv.* **5**, eaau7423 (2019).

[33] Q.-L. Lei and R. Ni, *Proceedings of the National Academy of Sciences* **116**, 22983 (2019).

[34] M. Huang, W. Hu, S. Yang, Q.-X. Liu, and H. Zhang, *Proceedings of the National Academy of Sciences* **118**, e2100493118 (2021).

[35] B. Zhang and A. Snejhko, *Physical Review Letters* **128**, 218002 (2022).

[36] N. Oppenheimer, D. B. Stein, M. Y. B. Zion, and M. J. Shelley, *Nature communications* **13**, 804 (2022).

[37] D. Hexner and D. Levine, *Physical review letters* **118**, 020601 (2017).

[38] D. Hexner, P. M. Chaikin, and D. Levine, *Proceedings of the National Academy of Sciences* **114**, 4294 (2017).

[39] J. H. Weijs and D. Bartolo, *Physical review letters* **119**, 048002 (2017).

[40] S. Wilken, A. Z. Guo, D. Levine, and P. M. Chaikin, *arXiv preprint arXiv:2212.09913* (2022).

[41] M. Floreescu, S. Torquato, and P. J. Steinhardt, *Proc. Natl. Acad. Sci. U.S.A.* **106**, 20658 (2009).

[42] M. A. Klatt, P. J. Steinhardt, and S. Torquato, *Proceedings of the National Academy of Sciences* **119**, e2213633119 (2022).

[43] G. Zhang, F. H. Stillinger, and S. Torquato, *J. Chem. Phys.* **145**, 244109 (2016).

[44] D. Chen and S. Torquato, *Acta Mater.* **142**, 152 (2018).

[45] S. Torquato, *Physical Review E* **104**, 054102 (2021).

[46] Y. Xu, S. Chen, P. Chen, W. Xu, and Y. Jiao, *Phys. Rev. E* **96**, 043301 (2017).

[47] O. Leseur, R. Pierrat, and R. Carminati, *Optica* **3**, 763 (2016).

[48] S. Yu, *Nature Computational Science* **3**, 128 (2023).

[49] H. Mizuno, H. Shiba, and A. Ikeda, *Proceedings of the National Academy of Sciences* **114**, E9767 (2017).

[50] Y.-C. Hu and H. Tanaka, *Nature Physics* **18**, 669 (2022).

[51] D. Xu, S. Zhang, H. Tong, L. Wang, and N. Xu, *Nature Communications* **15**, 1424 (2024).

[52] Y. Wang, Z. Qian, H. Tong, and H. Tanaka, *Nature Communications* **16**, 1398 (2025).

[53] H. Zhuang, D. Chen, L. Liu, D. Keeney, G. Zhang, and Y. Jiao, *Journal of Physics: Condensed Matter* **36**, 285703 (2024).

[54] T. Lubensky, C. Kane, X. Mao, A. Souslov, and K. Sun, *Reports on Progress in Physics* **78**, 073901 (2015).

[55] X. Mao and T. C. Lubensky, *Annual Review of Condensed Matter Physics* **9**, 413 (2018).

[56] F. R. K. Chung, *Spectral Graph Theory*, vol. 92 of *CBMS Regional Conference Series in Mathematics* (American Mathematical Society, 1997).

[57] P. G. Doyle and J. L. Snell, *Random Walks and Electric Networks*, no. 22 in Carus Mathematical Monographs (Mathematical Association of America, 1984).

[58] N. W. Ashcroft and N. D. Mermin, *Solid State Physics* (Holt, Rinehart and Winston, 1976).

[59] I. M. Lifshitz, S. A. Gredeskul, and L. A. Pastur, *Introduction to the Theory of Disordered Systems* (Wiley, 1988).

[60] M. Belkin and P. Niyogi, in *Advances in Neural Information Processing Systems* (2007).

[61] N. G. Trillos and D. Slepčev, *Applied and Computational Harmonic Analysis* **45**, 239 (2018).

[62] K. Adhikari, R. J. Adler, O. Bobrowski, and R. Rosenthal, *The Annals of Applied Probability* **32**, 1734 (2022).

[63] M. Reed and B. Simon, *Methods of Modern Mathematical Physics, Vol. IV: Analysis of Operators* (Academic Press, 1978).

[64] A. Böttcher and B. Silbermann, *Introduction to Large Truncated Toeplitz Matrices* (Springer, 1999).

[65] C. Kittel and P. McEuen, *Introduction to solid state physics* (John Wiley & Sons, 2018).

[66] S. Timoshenko and S. Woinowsky-Krieger (1959).

[67] D. L. Nika and A. A. Balandin, *Reports on Progress in Physics* **80**, 036502 (2017).

[68] R. D. Batten, F. H. Stillinger, and S. Torquato, *J. Appl. Phys.* **104**, 033504 (2008).